Nailing down the slip rate of the Altyn Tagh fault

Jiankun He, Philippe Vernant, Jean Chery, Weimin Wang, Shuangjiang Lu, Wenfei Ku, Wenhai Xia, Roger Bilham

Nailing down the slip rate of the Altyn Tagh fault

Jiankun He,[1] Philippe Vernant,[2] Jean Chéry,[2] Weimin Wang,[1] Shuangjiang Lu,[1] Wenfei Ku,[3] Wenhai Xia,[4] and Roger Bilham[5]

Received 27 July 2013; revised 28 September 2013; accepted 5 October 2013; published 23 October 2013.

[1] Previous estimates of the geodetic and geologic slip rates of the 1500 km long Altyn Tagh fault bordering the northern edge of the Tibetan plateau vary by a factor of five. Proposed reasons for these discrepancies include poor GPS geometry, interpretative errors in terrace morphology, and changes in fault slip rate over time. Here we present results from a new dense GPS array orthogonal to the fault at ~86.2°E that indicates a velocity of $9.0^{-3.2}/_{+4.4}$ mm/yr, in close agreement with geomorphologic estimates at the same location. Our estimated geodetic slip rate is consistent with recent geological slip rates based on terrace offsets. The resulting mean combined geological and geodetic slip rate (9.0 ± 4.0 mm/yr) is remarkably uniform for the central ~800 km of the Altyn Tagh fault, significantly lower than early kinematic estimates and consistent with deformation elsewhere in Tibet and central Asia. **Citation:** He, J., P. Vernant, J. Chéry, W. Wang, S. Lu, W. Ku, W. Xia, and R. Bilham (2013), Nailing down the slip rate of the Altyn Tagh fault, *Geophys. Res. Lett.*, *40*, 5382–5386, doi:10.1002/2013GL057497.

1. Introduction

[2] The slip rate of the Altyn Tagh fault (Figure 1a) is central to kinematic description of the Himalayan collision process from India to Mongolia [*Molnar and Tapponnier*, 1975; *Avouac and Tapponnier*, 1993; *Houseman and England*, 1993; *Peltzer and Saucier*, 1996; *England and Molnar*, 1997; *Tapponnier et al*., 2001; *Gold et al*., 2009], yet despite its prominent morphological expression, considerable debate has attended quantifying its velocity [*Peltzer et al*., 1989; *Bendick et al*., 2000; *Mériaux et al*., 2004; *Zhang et al*., 2004; *Mériaux et al*., 2005; *Cowgill*, 2007; *Zhang et al*., 2007; *Mériaux et al*., 2012]. This is partly due to disagreements in interpretations of the age and offset of geological markers, and partly due to internal deformation within Tibet that adds uncertainty to geodetic interpretations of slip rate using GPS methods. Attempts to reconcile reported velocities include the possibility that changes of rate have occurred over the past several thousands of years [*Washburn et al*., 2001; *Wallace et al*., 2004], or that possible spatial variations in elastic loading and fault friction exist [*Chéry and Vernant*, 2006]. The highest estimates of velocity (~30 mm/yr) [*Peltzer et al*., 1989; *Mériaux et al*., 2004] would accommodate more Indo-Asian convergence than the Himalaya [*Lavé and Avouac*, 2000], leaving negligible convergence to explain deformation within Tibet and NE Asia. In contrast, the lowest estimates (~6 mm/yr) [*Zhang et al*., 2004; *Meade*, 2007] would require higher slip rates on some faults within the Tibetan plateau (such as the Karakorum-Jiali fault) than is observed [*Chen et al*., 2004]. Geodetic measurements indicating that the Altyn Tagh fault slips at ~10 mm/yr [*Bendick et al*., 2000; *Wallace et al*., 2004; *Shen et al*., 2001] have been used to support continuum deformation of the Tibetan plateau [*Zhang et al*., 2004; *Houseman and England*, 1993; *England and Molnar*, 1997; *England and Molnar*, 2005], or block like deformation [*Meade*, 2007; *Thatcher*, 2007], however, geodetic measurements across the fault have not been measured in the same places as geologic slip rates. Moreover, due to the difficulty in accessing this remote region, previous GPS measurements crossing the northern edge of the Tibetan plateau are sparse and have spanned ~300 km [*Bendick et al*., 2000] to ~1000 km [*Shen et al*., 2001] along strike, possibly sampling differences in slip rate [*Mériaux et al*., 2004; *Mériaux et al*., 2005].

[3] The highest published geological slip rate (26.9 ± 6.9 mm/yr) [*Mériaux et al*., 2004] has been reported from longitude 86.4°E where detailed measurements of riser offsets of different geomorphic terraces, using radiocarbon and ^{10}Be-^{26}Al cosmic ray exposure dating of the offset terraces, have provided a millennial slip rate for the fault [*Mériaux et al*., 2004; *Mériaux et al*., 2005; *Cowgill*, 2007; *Gold et al*., 2009; *Xu et al*., 2005]. In order to compare geodetic and geologic slip rate estimates, we have established a GPS profile as close as possible to the site of *Mériaux et al*. [2004].

2. Data

[4] In 2009, we established a 400 km long GPS profile perpendicular to the Altyn Tagh fault crossing the fault at ~86.2°E (Figure 1b). Seventeen GPS benchmarks with forced antenna centering and an average spacing of 10–20 km were measured 2–3 times between 2009 and 2011, using Trimble NetRS receivers with Zephyr antennae. Observation times for all sites exceeded 48 h during each survey. The GPS data were processed with GAMIT/GLOBK software [*Herring et al*., 2010] and rotated from the International Terrestrial Reference Frame 2008 (ITRF2008) to a Tarim reference frame by minimizing the velocities of the sites AT12, AT13, and AT16 (Figure 1b). Following *Reilinger et al*. [2006], we use the "real sigma" algorithm to account for the correlated errors in the time series by calculating a unique noise model for each

[1]Key Laboratory of Continental Collision and Plateau Uplift, Institute of Tibetan Plateau Research, Chinese Academy of Sciences, Beijing, China.
[2]Laboratoire Géosciences Montpellier UMR5243, CNRS Université de Montpellier II, Montpellier, France.
[3]Department of Geological Sciences, University of Missouri, Columbia, Missouri, USA.
[4]Department of Survey Engineering, Xi'an University of Science and Technology, Xi'an, China.
[5]CIRES and Department of Geological Sciences, University of Colorado, Boulder, Colorado, USA.

Corresponding author: J. He, Key Laboratory of Continental Collision and Plateau Uplift, Institute of Tibetan Plateau Research, Chinese Academy of Sciences, Beijing 100029, China. (jkhe@itpcas.ac.cn)

0094-8276/13/10.1002/2013GL057497

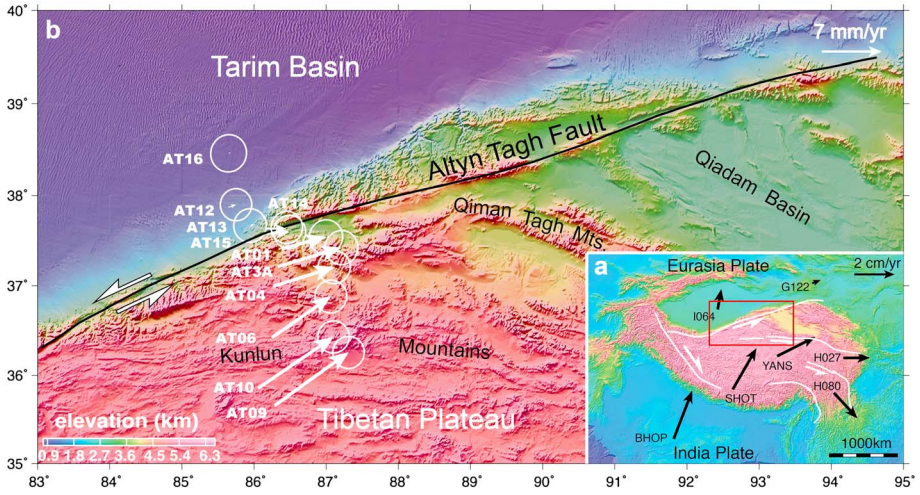

Figure 1. Tectonic setting of the Altyn Tagh fault superimposed on relief map. (a) A simplified view of strike-slip faults around the Tibetan plateau and their deformation sense associated with the current GPS velocity field relative to Eurasia [*Zhang et al*., 2004]. Red squared region is the location of Figure 1b. (b) Detailed topographic map around the central portion of the Altyn Tagh fault and GPS velocities relative to the Tarim basin with uncertainties plotted at 95% confidence level.

continuous GPS station. Since our sites are only measured episodically, we use the average value of correlated noise model values determined for 320 continuous GPS stations globally distributed with time series spans ranging from 2.5 to 17 years. Hence, we apply a 1-mm/√yr random walk stochastic noise to the survey GPS horizontal time series estimates. One sigma velocity uncertainties are ≤0.9 mm/yr (Table 1). The surface active fault is located 200 m north of the point AT15 (Figure 1b).

[5] In Figure 2a, we show GPS velocities and topography plotted orthogonal to the fault at 86.18°N and 37.58°E. If outliers are ignored, the data indicate that shear strain caused by slip of the fault at depth is concentrated within a 60 km zone, centered some 15 km south of the surface fault (Figure 2b). Post-seismic signals of the 1999 M_w 7.9 Manyi earthquake may perturb our southernmost two GPS stations, that are <100 km from its surface rupture, but interferometric synthetic aperture radar (InSAR) measurements show that

Table 1. GPS Site Velocities and 1σ Uncertainties[a]

Site	Lon. (°N)	Lat. (°E)	$V_{E(TARIM)}$ (mm/yr)	$V_{N(TARIM)}$ (mm/yr)	$V_{E(ITRF08)}$ (mm/yr)	$V_{N(ITRF08)}$ (mm/yr)	σ_E (mm/yr)	σ_N (mm/yr)	Corr.
AT01	86.380	37.413	5.48	1.44	32.09	11.70	0.84	0.87	0.021
AT02	86.327	37.336	7.38	1.59	33.93	11.91	0.82	0.84	0.017
AT03A	86.333	37.213	7.81	2.36	34.26	12.67	0.83	0.86	0.011
AT03	86.309	37.232	10.61	1.81	37.07	12.14	0.79	0.81	0.008
AT04	86.264	36.994	7.52	2.37	33.80	12.76	0.81	0.83	0.013
AT05	86.317	36.575	3.45	1.30	29.40	11.68	0.84	0.86	0.022
AT06	86.250	36.428	7.24	5.02	33.06	15.46	0.80	0.82	0.013
AT07	86.056	36.253	5.74	5.41	31.41	16.04	0.79	0.81	0.011
AT08	86.119	36.026	8.94	2.45	34.43	13.04	0.79	0.81	0.007
AT09	86.283	35.657	9.13	6.58	34.34	17.05	0.79	0.81	0.003
AT10	86.056	35.853	9.29	6.35	34.65	17.01	0.79	0.81	0.007
AT11	86.292	35.376	3.85	5.36	28.83	15.84	0.81	0.83	0.009
AT12[b]	85.646	37.871	0.93	0.31	27.86	11.21	0.79	0.81	0.005
AT13[b]	86.011	37.681	−0.59	−0.14	26.21	10.44	0.82	0.85	0.005
AT14	86.167	37.620	2.53	0.08	29.30	10.53	0.81	0.84	0.004
AT15	86.176	37.581	2.81	0.19	29.55	10.63	0.81	0.84	0.002
AT16[b]	85.677	38.466	−0.26	−0.08	27.14	10.77	0.90	0.94	0.025
BJFS	115.892	39.609	8.03	6.61	33.02	−11.53	0.50	0.61	0.209
GUAO	87.177	43.471	0.58	−2.83	32.00	6.40	0.57	0.74	−0.030
HYDE	78.551	17.417	29.59	15.86	40.21	34.59	0.52	0.52	−0.072
IISC	77.570	13.021	34.78	14.90	42.14	34.90	1.26	0.81	0.091
IRKT	104.316	52.219	−13.97	0.61	23.99	−7.19	0.53	0.55	−0.050
KIT3	66.885	39.135	0.14	−21.05	24.38	5.64	0.58	0.86	−0.108
LHAZ	91.104	29.657	27.01	11.94	47.29	18.58	1.57	0.67	−0.031
POL2	74.694	42.680	−2.85	−16.05	25.93	4.38	0.53	0.86	−0.096
SELE	77.017	43.179	−1.86	−13.74	27.80	4.69	0.53	0.59	−0.119
TASH	69.296	41.328	5.52	−24.17	31.92	0.68	0.53	0.95	−0.126
ULAB	107.052	47.865	−4.95	1.22	29.14	−9.09	0.59	0.80	−0.005
URUM	87.601	43.808	0.26	−3.55	31.97	5.27	0.60	0.95	−0.018
XIAN	109.222	34.369	31.86	−17.87	53.92	−28.93	0.84	0.89	0.036

[a]Longitude (Lon.) and latitude (Lat.) are given in degrees east and north, respectively. Velocities and uncertainties are given in mm.yr^{-1}.
[b]The Tarim reference frame is determined by minimizing the horizontal velocities of the three sites on the stable Tarim block (AT12, AT13, and AT16).

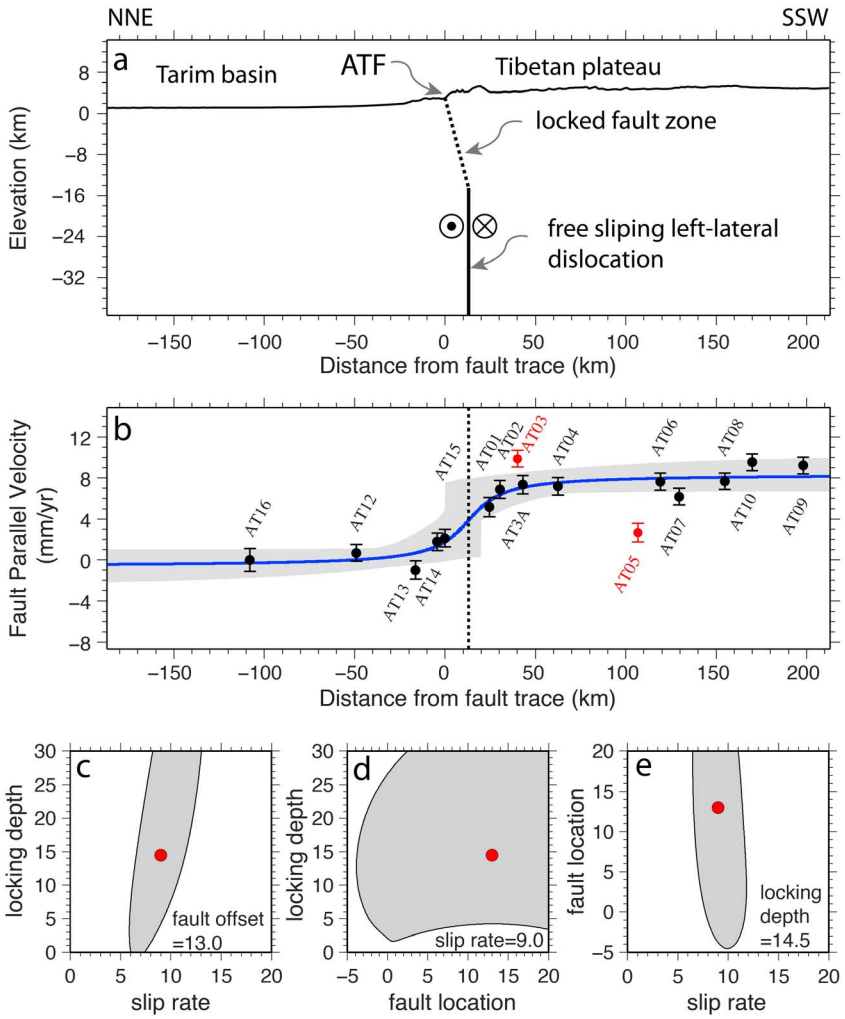

Figure 2. Sections along the azimuth of 155° across the Altyn Tagh fault at 86.176°E, 37.581°N. (a) Topographic variation normal to the Altyn Tagh fault along the profile and intersismic deformation model of the Altyn Tagh fault, assuming that the fault is a vertical plane creeping at uniform rate below an elastic half space. (b) Fault-parallel velocity component of the GPS measurements. Error bars represent 1σ uncertainty of the GPS velocities relative to Tarim basin, best fit model using an elastic dislocation (blue dotted line), and all the possible models based on the uncertainties (95% confidence, light grey area). (c) Uncertainties for locking depth versus strike-slip rate for the best dislocation offset of 13 km. (d) Uncertainties for locking depth versus dislocation offset for the best strike-slip rate of 9 mm/yr. (e) Uncertainties for dislocation offset versus strike-slip rate for the best locking depth of 14.5 km.

most post-seismic deformation is within ~20 km of the surface rupture and that the surface displacement following the earthquake obeys an exponential decay with time [*Ryder et al.*, 2007]. Hence, the Manyi earthquake postseismic signal contributes little (<1%) to the interpretation of the Altyn Tagh shear signal. By assuming that the overall velocity field is related to steady state creep of the Altyn Tagh fault below its locking depth (Figure 2a), we can use elastic dislocation theory [*Savage and Burford*, 1973] to calculate fault slip rate and locking depth.

3. Results and Discussion

[6] The best fitting solution is obtained with a strike-slip rate of 9.0 mm/yr, a locking depth of 14.5 km, and a dislocation offset 13 km south of the surface fault (Figure 2b). We use the F-ratio test designed by *DeMets* [1992] specifically to compare the fit of the two Euler poles to a set of directional data. In this study, we compare the fit of the fault parameters obtained with a forward model to a set of GPS velocity vectors. Using a 95% confidence level as the cutoff for significant differences, the uncertainty on the slip rate is −3.2 and +4.4 mm/yr. We note that our strike-slip-velocity estimate is independent of the locking depth or offset, which are poorly constrained (Figures 2c–2e). The apparent asymmetry of the shear strain relative to the surface fault (Figures 2a and 2b) is intriguing and is similar to results reported from InSAR measurements ~150 km west [*Elliott et al.*, 2008] and ~800 km east [*Jolivet et al.*, 2008] of our profile. Several mechanisms can explain the asymmetry of the interseismic velocity: rheological contrast on two sides of the Altyn Tagh fault, a variation of the elastic crustal thickness [*Jolivet et al.*, 2008], or a southerly dip to the fault. An insignificant step in velocity can be discerned between sites AT04 and AT10, which span the approximate western projection of the Kunlun fault [*Tapponnier et al.*, 2001]. If sites south of AT04 are omitted

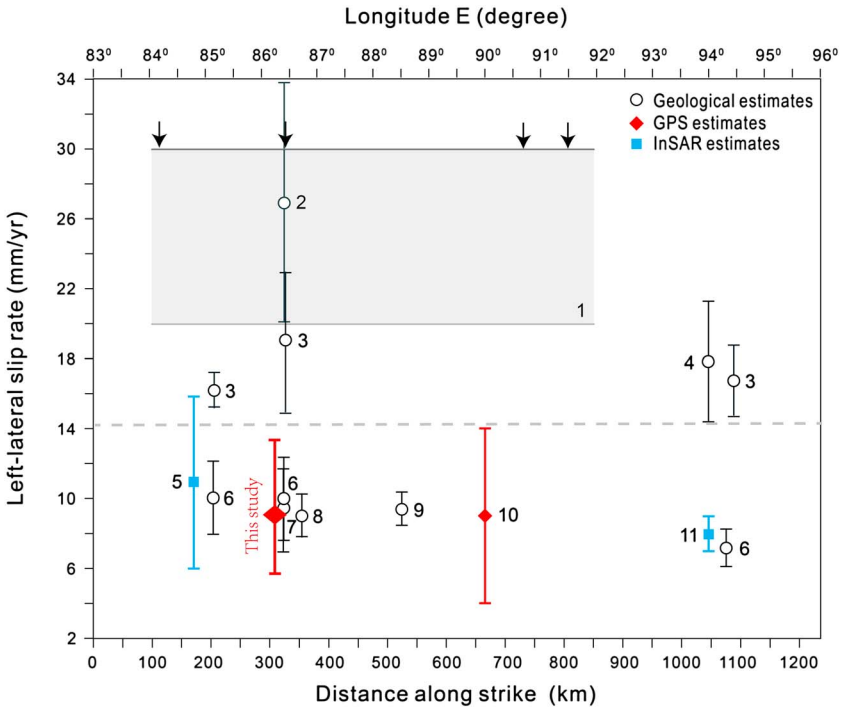

Figure 3. Geologic (black), InSAR (blue), and geodetic slip rates (red) estimated along the Altyn Tagh fault. Error bar represents 1σ uncertainty. The five published geologic slip rates above the dashed line were assumed that the riser offset corresponds to the age of the lower terrace abandonment [*Mériaux et al*., 2004; *Mériaux et al*., 2005; *Xu et al*., 2005]. The six published geologic slip rates below the dashed line were assumed that the riser offsets correspond to age of abandonment of the higher terrace [*Cowgill*, 2007; *Zhang et al*., 2007; *Cowgill et al*., 2009; *Gold et al*., 2009]. Slip rates in the shaded area assumed that the fault offsets (at arrowed places) were formed ~10 ± 2 ka ago [*Peltzer et al*., 1989]; to bring them into line with the revised velocity for the fault (~9 mm/yr), the assumed age would need to be considerably older. Data are from (1) *Peltzer et al*. [1989], (2) *Mériaux et al*. [2004], (3) *Xu et al*. [2005], (4) *Mériaux et al*. [2005], (5) *Elliott et al*. [2008], (6) *Zhang et al*. [2007], (7) *Cowgill* [2007]; (8) *Gold et al*. [2009], (9) *Cowgill et al*. [2009], (10) *Bendick et al*. [2000], and (11) *Jolivet et al*. [2008].

from our solution, a value of $7.9^{-2.7}/_{+3.4}$ mm/yr is obtained for the Altyn Tagh fault, within the uncertainty obtained from the best fitting solution using all the data.

[7] We note that our slip rate ($9.0^{-3.2}/_{+\ 4.4}$ mm/yr) is in good agreement with the 9.4 ± 2.3 mm/yr slip rate estimated 25 km east of our profile [*Cowgill*, 2007], where offsets of fluvial terraces were previously interpreted to signify a slip rate of 26.9 ± 6.9 mm/yr [*Mériaux et al*., 2004]. The low geological rate [*Cowgill*, 2007; *Zhang et al*., 2007] assumes that offset started immediately after the abandonment of the upper terraces, whereas the high rate [*Mériaux et al*., 2004; *Mériaux et al*., 2005; *Xu et al*., 2005] follows from assuming that offset of fluvial terrace risers corresponds to the time of the abandonment of the lower terrace, an interpretation that we now suggest may be discarded. Thus, if we apply a similar interpretation to offset terraces in other locations along the fault where high rates have been reported [*Cowgill*, 2007; *Gold et al*., 2009; *Cowgill et al*., 2009], we find that rates estimated by correlating the riser offsets to the time of upper terrace abandonment are comparable to the geodetic slip rates estimated from InSAR and GPS measurements (Figure 3). The resulting conformity between geodetic and revised geologic slip rates leads us to conclude that all the slip rate estimates of the Altyn Tagh fault [*Bendick et al*., 2000; *Mériaux et al*., 2004; *Wallace et al*., 2004; *Zhang et al*., 2004; *Mériaux et al*., 2005; *Cowgill*, 2007; *Zhang et al*., 2007; *Elliott et al*., 2008; *Jolivet et al*., 2008; *Cowgill et al*., 2009] can be reconciled with an almost uniform slip rate of ~9 mm/yr along much of the fault.

4. Conclusions

[8] When combined with previous GPS estimates [*Bendick et al*., 2000; *Wallace et al*., 2004; *Zhang et al*., 2004], our new results suggest a remarkably uniform slip rate of ~9 mm/yr along the central ~800 km between 85°E and 94°E of the Altyn Tagh fault. At the eastern end of the fault near the Qilian Shan, the slip rate decreases from ~10 mm/yr to ~1.6 mm/yr [*Gan et al*., 2007]. The uniform slip relative to the rigid Tarim Basin to the north suggests that negligible deformation is accommodated by the Qiman Tagh Mountains and the western Qiadam basin (Figure 1b). An inferred Indo-Asian convergence direction of N11°E [*Zhang et al*., 2004] near the central Altyn Tagh indicates that the fault absorbs approximately 5 mm/yr of the 37 mm/yr overall convergence. Approximately, 30–50% of the Indo-Asian convergence is absorbed across the Himalaya [*Chen et al*., 2004; *Zhang et al*., 2004], leaving a significant amount of Indio-Asia convergence to be accommodated by contraction of the Tibetan Plateau [*Houseman and England*, 1993; *Zhang et al*., 2004] and by deformation in northeast Asia [*Calais et al*., 2003]. Therefore, our apparent uniform slip rate suggests that the surface carapace of the northern Tibetan plateau moves coherently, consistent with block-like motion of the plateau [*Meade*, 2007; *Thatcher*, 2007].

[9] **Acknowledgments.** We thank Xiongwen Zhang, Dexiao Wu, Jing Wang, and Jiang Lu from Xingjiang Exploration and Climbing Association for the field logistic assistance. We thank Jeff Freymueller and one anonymous reviewer for their thoughtful comments. This work was jointly funded by NSF and CAS of China (41030320, KZCX2-EW-116) and the French ANR grant (ANR-07-JCJC-0015).

[10] The Editor thanks Jeffrey Freymueller and an anonymous reviewer for their assistance in evaluating this paper.

References

Avouac, J.-P., and P. Tapponnier (1993), Kinematic model of active deformation in central Asia, *Geophys. Res. Lett.*, *20*, 895–898.

Bendick, R., P. Bilham, J. T. Freymueller, K. M. Larson, and G. Yin (2000), Geodetic evidence for a low slip rate in the Altyn Tagh fault system, *Nature*, *386*, 61–64.

Calais, E., M. Vergnolle, V. San'kov, A. Lukhnev, A. Miroshnitchenko, S. Amarjargal, and J. De´verche`re (2003), GPS measurements of crustal deformation in the Baikal-Mongolia area (1994–2002): Implications for current kinematics of Asia, *J. Geophys. Res.*, *108*(B10), 2501, doi:10.1029/2002JB002373.

Chen, Q., J. T. Freymueller, Q. Wang, Z. Yang, C. Xu, and J. Liu (2004), A deforming block model for the present-day tectonics of Tibet, *J. Geophys. Res.*, *109*, B01403, doi:10.1029/2002JB002151.

Chéry, J., and P. Vernant (2006), Lithospheric elasticity promotes episodic fault activity, *Earth Planet. Sci. Lett.*, *243*, 211–217.

Cowgill, E. (2007), Impact of riser reconstructions on estimation of secular variation in rates of strike-slip faulting: Revisiting the Cherchen River site along the Altyn Tagh fault, NW China, *Earth Planet. Sci. Lett.*, *254*, 239–255.

Cowgill, E., R. D. Gold, X. H. Chen, X. F. Wang, J. R. Arrowsmith, and J. Southon (2009), Low Quaternary slip rate reconciles geodetic and geologic rates along the Altyn Tagh fault, northwestern Tibet, *Geology*, *37*(7), 647–650.

DeMets, C. (1992), Oblique convergence and deformation along the Kuril and Japan Trenches, *J. Geophys. Res.*, *97*, 17,615–17,625.

Elliott, J. R., J. Biggs, B. Parsons, and T. J. Wright (2008), InSAR slip rate determination on the Altyn Tagh Fault, northern Tibet, in the presence of topographically correlated atmospheric delays, *Geophys. Res. Lett.*, *35*, L12309, doi:10.1029/2008GL033659.

England, P., and P. Molnar (1997), Active deformation of Asia: From kinematics to dynamics, *Science*, *278*, 647–650.

England, P., and P. Molnar (2005), Late Quaternary to decadal velocity fields in Asia, *J. Geophys. Res.*, *110*, B12401, doi:10.1029/2004JB003541.

Gan, W., P. Zhang, Z.-K. Shen, Z. Niu, M. Wang, Y. Wan, D. Zhou, and J. Cheng (2007), Present-day crustal motion within the Tibetan Plateau inferred from GPS measurements, *J. Geophys. Res.*, *112*, B08416, doi:10.1029/2005JB004120.

Gold, R. D., E. Cowgill, J. R. Arrowsmith, J. Gosse, X. Chen, and X.-F. Wang (2009), Riser diachroneity, lateral erosion, and uncertainty in rates of strike-slip faulting: A case study from Tuzidun along the Altyn Tagh Fault, NW China, *J. Geophys. Res.*, *114*, B04401, doi:10.1029/2008JB005913.

Herring, T. A., R. W. King, and S. C. McClusky (2010), Introduction to GAMIT/GLOBK, Release 10.35, Massachussetts Institute of Technology, Cambridge, Mass.

Houseman, G., and P. England (1993), Crustal thickening versus lateral expulsion in the Indian-Asian continental collision, *J. Geophys. Res.*, *98*, 12,233–12,249.

Jolivet, R., R. Cattin, N. Chamot-Rooke, C. Lasserre, and G. Peltzer (2008), Thin-plate modeling of interseismic deformation and asymmetry across the Altyn Tagh fault zone, *Geophys. Res. Lett.*, *35*, L02309, doi:10.1029/2007GL031511.

Lavé, J., and J. P. Avouac (2000), Active folding of fluvial terraces across the Siwaliks Hills, Himalayas of central Nepal, *J. Geophys. Res.*, *105*, 5735–5770.

Meade, J. (2007), Present-day kinematics at the India-Asia collision zone, *Geology*, *35*, 81–84.

Mériaux, A. S., F. J. Ryerson, P. Tapponnier, J. Van der Woerd, R. C. Finkel, X. Xu, Z. Xu, and M. W. Caffee (2004), Rapid slip along the central Altyn Tagh Fault: Morphochronologic evidence from Cherchen He and Sulamu Tagh, *J. Geophys. Res.*, *109*, B06401, doi:10.1029/2003JB002558.

Mériaux, A. S., et al. (2005), The Aksay segment of the northern Altyn Tagh fault: Tectonic geomorphology, landscape evolution, and Holocene slip rate, *J. Geophys. Res.*, *110*, B04404, doi:10.1029/2004JB003210.

Mériaux, A. S., J. Van der Woerd, P. Tapponnier, F. J. Ryerson, R. C. Finkel, C. Lasserre, and X. Xu (2012), The Pingding segment of the Altyn Tagh Fault (91E), Holocene slip-rate determination from cosmogenic radionuclide dating of offset fluvial terraces, *J. Geophys. Res.*, *117*, B09406, doi:10.1029/2012JB009289.

Molnar, P., and P. Tapponnier (1975), Cenozoic tectonics of Asia: Effects of a continental collision, *Science*, *189*, 419–426.

Peltzer, G., and F. Saucier (1996), Present-day kinematics of Asia derived from geologic fault rates, *J. Geophys. Res.*, *101*, 27,943–27,956.

Peltzer, G., P. Tapponnier, and R. Armijo (1989), Magnitude of Late Quaternary left-lateral displacements along the north edge of Tibet, *Science*, *246*, 1285–1289.

Reilinger, R., et al. (2006), GPS constraints on continental deformation in the Africa-Arabia-Eurasia continental collision zone and implications for the dynamics of plate interactions, *J. Geophys. Res.*, *111*, B05411, doi:10.1029/2005JB004051.

Ryder, I., B. Parsons, T. J. Wright, and G. J. Funning (2007), Post-seismic motion following the 1997 Manyi (Tibet) earthquake: InSAR observations and modelling, *Geophys. J. Int.*, *169*, 1009–1027.

Savage, J. C., and R. O. Burford (1973), Geodetic determination of the relative plate motion in central California, *J. Geophys. Res.*, *78*, 832–845.

Shen, Z.-K., M. Wang, Y. X. Li, D. Jackson, A. Yin, D. Dong, and P. Fang (2001), Crustal deformation along the Altyn Tagh fault system, western China, from GPS, *J. Geophys. Res.*, *106*, 30,607–30,621.

Tapponnier, P., Z. Xu, F. Roger, B. Meyer, N. Arnaud, G. Wittlinger, and Y. Jingsui (2001), Oblique stepwise rise and growth of the Tibet plateau, *Science*, *294*, 1671–1677.

Thatcher, W. (2007), Microplate model for the present-day deformation of Tibet, *J. Geophys. Res.*, *112*, B01401, doi:10.1029/2005JB004244.

Wallace, K., G. Yin, and R. Bilham (2004), Inescapable slow slip on the Altyn Tagh fault, *Geophys. Res. Lett.*, *31*, L06613, doi:10.1029/2004GL019724.

Washburn, Z., J. R. Arrowsmith, S. L. Forman, E. Cowgill, W. Xiaofeng, Z. Yueqiao, and C. Zhengle (2001), Late Holocene Earthquake History of the Central Altyn Tagh Fault, China, *Geology*, *29*, 1051–1054.

Xu, X., et al. (2005), Late Quaternary sinistral slip rate along the Altyn Tagh fault and its structural transformation model, *Sci. China Ser. D Earth Sci.*, *48*, 384–397.

Zhang, P. Z., et al. (2004), Continuous deformation of the Tibetan Plateau from global positioning system data, *Geology*, *32*, 809–812.

Zhang, P., P. Molnar, and X. Xu (2007), Late Quaternary and present-day rates of slip along the Altyn Tagh Fault, northern margin of the Tibetan Plateau, *Tectonics*, *26*, TC5010, doi:10.1029/2006TC002014.